# Thermal release tape-assisted semiconductor membrane transfer process for hybrid photonic devices embedding quantum emitters

(Dated: 29 April 2022)

The ability to combine different materials enables a combination of complementary properties and device engineering that cannot be found or exploited within a single material system. In the realm of quantum nanophotonics, one might want to increase device functionality by, for instance, combining efficient classical and quantum light emission available in III-V semiconductors, low-loss light propagation accessible in silicon-based materials, fast electro-optical properties of lithium niobate, and broadband reflectors and/or buried metallic contacts for local electric field application or electrical injection of emitters. However, combining different materials on a single wafer is challenging and may result in low reproducibility and/or low yield. For instance, direct epitaxial growth requires crystal lattice matching for producing of defect-free films, and wafer bonding requires considerable and costly process development for high bond strength and yield. We propose a transfer printing technique based on the removal of arrays of free-standing membranes and their deposition onto a host material using a thermal release adhesive tape-assisted process. This approach is versatile, in that it poses limited restrictions on the transferred and host materials. In particular, we transfer 190 nm-thick GaAs membranes that contain InAs quantum dots and which have dimensions up to about $260\,\mu\text{m} \times 80\,\mu\text{m}$ onto a gold-coated silicon substrate. We show that the presence of a back reflector combined with the etching of micropillars significantly increases the extraction efficiency of quantum light from a single quantum dot line, reaching photon fluxes exceeding $8 \times 10^5$ photons per second. This flux is four times higher than the highest count rates measured from emitters outside the pillars on the same chip. Given its versatility and ease of processing, this technique provides a path to realising hybrid quantum nanophotonic devices that combine virtually any material in which free-standing membranes can be made onto any host substrate, without specific compatibility issues and/or requirements.

The development of hybrid integrated photonic devices has attracted considerable interest, for instance in the field of silicon photonics, in order to realise III-V lasers on silicon[1] and light-emitting diodes on flexible substrates[2]. More recently, hybrid approaches have been investigated for quantum photonic applications[3,4]. There are several different approaches for realizing hybrid integration, including wafer bonding[6] and pick-and-place of nanophotonic devices[5]. These approaches have led to the successful demonstration of low-loss guidance of quantum light[5], cavity quantum electro-dynamics on a III-V/silicon platform[6], on-chip interference from quantum dots in silicon nanowires[7] and single-photon indistinguishability in hybrid devices[8]. An alternative route is represented by transfer printing, where devices or patches of material are transferred from one substrate to another, an approach that has been widely exploited in electronics[9–12], which has resulted in the realization of detectors and flexible devices[13–17], and has also more recently been applied to quantum nanophotonics[5,19–23]. The relative performance of quantum nanophotonic devices realized by these different integration technique has been recently reviewed in Ref. 4, for example, while Refs. [XX,YY] discuss different heterogeneous integration strategies being employed in the field of integrated photonics.

Here, we propose the use of a membrane-transfer technique for easy integration of different (and potentially multiple) materials on the same wafer. Our technique relies on a thermal-release tape that is commonly used to exfoliate two-dimensional materials[24,25] and we use it to integrate active quantum emitters on a host substrate. Compared to polydimethylsiloxane (PDMS)-based processes, our approach replaces the patterning and kinetic control of adhesion required when utilizing elastic stamps with membrane release that is controlled by the tape's temperature. Given the relatively large area of material deposited, compared to the footprint of standard nanophotonic structures, hundreds of devices can then be nanofabricated on the hybrid chip, for instance to control light emission and propagation.

The transfer process that we have developed is schematically illustrated in Fig. 1a. A direct laser write maskless aligner (equipped with a laser emitting at 405 nm) is used to write a series of apertures on a photoresist film ($\approx$1.6 $\mu$m thick), the holes appear as 'dashed lines' that define the perimeter of the membranes that will be transferred. These apertures are then dry-etched through the GaAs top layer to reach an underlying AlGaAs sacrificial layer. The residual resist is chemically removed with a solvent, and a hydrofluoridic acid wet etch (49 % concentration by mass in water) is used to undercut the membranes. The samples

are then cleaned in de-ionised water and isopropyl alcohol and dried by heating to about 120 °C. A resist layer is then spin coated on the chip (≈150 nm of PMMA 495A4 ) to protect the GaAs from impurities during the transfer process that is carried out by slowly, manually placing a thermal release tape (Graphene Supermarket GTT-DS ) on the sample surface (see Fig. 1b). The tape, that now has the membranes attached, is then manually removed and placed on a host substrate. The sample is then slowly heated up to about 100 °C so that the tape loses adhesion and leaves the membranes on the host substrate where they are held in place, by van der Waals forces. Finally, the resist layer that protected the GaAs membrane is chemically removed with a solvent (Microposit remover 1165, Rohm and Haas ) that does not etch the GaAs membrane. It is worth noting that without the resist protective layer, the adhesive tape would leave residues on the sample surface that can be difficult to remove and that can affect the optical quality of the fabricated devices. The presence of the PMMA reduces the yield in the pick up process but guarantees cleanliness of the membrane top surface (see Fig. 1b).

Figure 1b shows examples of membranes of different sizes and shapes that we have transferred using the technique presented above. Arrays of hundreds of membranes can be transferred in one single step, in our case from samples as large as 2 cm × 2 cm (larger samples might be possible, but have not been tested), and the yield, defined as the number of transferred membranes that have more than 80 % of usable area, is generally around 75 %. Other approaches, for instance those based on PDMS as material to pick up the devices[5], require fine control on how the polymeric stamp is placed on the sample surface and how it is peeled off to release the transferred material. Our technique, instead, takes advantage of the fact that the tape has very strong adhesion until it is heated above a certain temperature, after which it will lose adhesion and it will release the vast majority of the membranes (more than about 90 %). A disadvantage is related to the need to protect the sample surface, in our case with a resist layer, which, as discussed above, can reduce the adhesion and therefore overall yield of the transfer process. Compared to wafer-bonding approaches[6], our transfer process is much more tolerant of surface roughness, eliminates time-consuming substrate removal steps, and materials can be directly bonded together without requiring intermediate matching layers.

We use this process to transfer 190 nm-thick GaAs membranes containing a layer of InAs quantum dots 95 nm below the sample surface and grown by molecular beam epitaxy

with a Stranski-Krastanov technique. As discussed, this membrane transfer process allows combinations of materials that can not be grown with the same techniques and/or in the same growth or deposition chambers. In this case, we deposit the GaAs membrane on a gold-coated silicon wafer and use the metal as a broadband back reflector. The presence of the back reflector alone (without any other fabricated devices) increases the amount of light collected above the sample by about a factor two, compared to the as-grown quantum dot emission. Figure 2 shows finite-difference time-domain simulations of the system under study, namely, an oscillating dipole within the GaAs membrane and on top of a gold layer. Panels (a,b) show the profile of the emitted intensity and panels (c,d) show how, by etching a micro-pillar of 1 $\mu$m of diameter, centered around the emitter, the light otherwise trapped within the membrane can now be guided vertically out of the chip (and towards an external collection objective or optical fiber). Patterning of the sample surface has also been used to increase the efficiency in light-emitting diodes[26]. Figure 2(e) shows examples of micro-pillars fabricated by electron-beam lithography, followed by argon ion milling, on the sample under study. The ion milling is used to avoid contamination of dry etcher chambers, due to the presence of the gold layer underneath the GaAs membrane, and a secondary ion mass spectrometry endpoint detector is used to stop the etching once the gold layer is reached.

We then characterise the emission properties of the quantum dots by means of micro-photoluminescence spectroscopy (a schematic of the set-up can be found in[27]). Figure 3 shows examples of photoluminescence emission spectra collected from quantum dots within micropillars (a) and in the unpatterned bulk material (b), for different laser excitation powers. The spectra show that the brightness is enhanced when the emitters are placed within the pillars. This is further demonstrated in Figure 3(c), where the intensity of selected quantum dot emission lines from panels (a) and (b) is plotted as a function of laser excitation power. We observe a clear enhancement in the collected intensity of the quantum dot emission lines, as shown in Fig. 3(a-c), when the emitters are located within the pillars, compared to the case where only the back reflector is present. This is due to the channelling of part of the light that would otherwise propagate in the plane towards the collection optics above the pillars, as shown in the simulations on Fig. 2. In the histograms in Fig. 3(d), the intensity collected when the emission of single quantum dot lines reaches the saturation level is plotted for about 150 quantum dot lines (within and outside the pillars): the distributions show the statistics of the enhancement in the brightness due to

the presence of the pillar structure, further proving the effectiveness of the device geometry under study. The histograms are fitted with log-normal distributions that peak at $7.5 \times 10^4$ photons per second and $23 \times 10^4$ photons per second, respectively, and count rates as high as $8 \times 10^5$ photons per second are recorded. In a similar system, where quantum dots are placed 95 nm away from a gold back-reflector, it was shown that no modification of the spontaneous emission lifetimes is obtained[27]. As in that previous work, no cavity-mediated effects are observed from the micropillars we study here, which instead acts as waveguides that guided the light towards the collection optics, as shown in Fig. 2. Therefore, the increase in brightness is attributed to the upwards guidance of the light thanks to the reflection at the gold layer and the mode confinement due to the micropillar geometry, not to a reduction of the emission lifetimes. From our simulations, quantum dots should be placed closer ($\lesssim$ 20 nm) to the metallic features for Purcell enhancement to be obtained (work in this direction is in progress[28]).

These results show how a simple pillar/back reflector geometry, made possible by the implementation of the transfer technique that we have developed, can increase the collection efficiency from single quantum dot lines. Other device geometries can be realised using this technique, for instance circular Bragg grating cavities with a gold back reflector[29], planar antennas[30], plasmonic structures[31], in an easy and repeatable manner.

In conclusion, we have shown how a technique based on thermal release adhesive tape can be used to pick up and deposit membranes onto host substrates, with an easy and versatile process that is transferred- and host-material independent. We have used this approach to transfer GaAs membranes containing InAs quantum dots onto a metal back reflector layer and we have shown how, combining the broadband reflection of gold with the fabrication on micro-pillars, we can enhance the collection efficiency of quantum light out of the chip. We foresee that this approach will allow the realisation of hybrid devices for classical and quantum photonics, taking advantage of the possibility of stacking relatively large areas of different materials and carrying out nano-fabrication processes on the final layered stack (or on each layer after transfer), without requiring very accurate pick-and-place processes of nano-photonic devices.

## REFERENCES


[1]S. Chen et al., Nature Photonics **10**, 307 (2016).

[2]S.-I. Park, Y. Xiong, R.-H. Kim et al., Science **325**, 977 (2009).

[3]A.W. Elshaari, W. Pernice, K. Srinivasan, O. Benson, V. Zwiller, Nature Photonics **14**, 285 (2020).

[4]J.-H. Kim, S. Aghaeimeibodi, J. Carolan, D. Englund, E. Waks, Optica **7**, 291 (2020).

[5]R. Katsumi, Y. Ota, M. Kakuda, S. Iwamoto, Y. Arakawa, Optica **5**, 691 (2018).

[6]M. Davanco, J. Liu, L. Sapienza, C.-Z. Zhang, J.V. De Miranda Cardoso, V. Verma, R. Mirin, S.W. Nam, L. Liu, K. Srinivasan, Nature Communications **8**, 889 (2017).

[7]A.W. Elshaari et al., Nature Communications **8**, 379 (2017).

[8]P. Schnauber et al., Nano Lett. **19**, 7164 (2019).

[9]E. Yablonovitch, T. Gmitter, J.P. Harbison, R. Bhat, Appl. Phys. Lett. **51**, 2222 (1987).

[10]C.-W. Cheng, K.-T. Shiu, N. Li, S.-J. Han, L. Shi, D.K. Sadana, Nature Communications **4**, 1577 (2013).

[11]A. Carlson, A.M. Bowen, Y. Huang, R.G. Nuzzo, J.A. Rogers, Adv. Mater. **24**, 5284 (2012).

[12]M.A. Meitl, Z.-T. Zhu, V. Kumar et al., Nature Materials **5**, 33 (2006).

[13]K. Sim et al., Scientific Reports **5**, 16133 (2015).

[14]Y.G. Sun, J.A. Rogers, Nano Letters **4**, 1953 (2004).

[15]M.A. Meitl et al., Nature Materials **5**, 33 (2006).

[16]C.H. Lee, D.R. Kim, X. Zheng, Proceedings of the National Academy of Sciences of the United States of America **107**, 9950 (2010).

[17]C. Linghu, S. Zhang, C. Wang, J. Song, npj Flexible Electronics **2**, 26 (2018).

[18]Z. Yan, T. Pan, M. Xue et al., Adv. Sci. **4**, 1700251 (2017).

[19]X. Wu et al., Nano Letters **17**, 4291 (2017).

[20]D. Jevtics et al., Optical Materials Express **11**, 3567 (2021).

[21]N.H. Wan, T.-J. Lu, K.C. Chen, et al., Nature **583**, 226 (2020).

[22]F. Peyskens, C. Chakraborty, M. Muneeb, D. Van Thourhout, D. Englund, Nature Communications **10**, 4435 (2019).

[23]P. Tonndorf, O. Del Pozo-Zamudio, N. Gruhler et al.,Nano Lett. **9**, 5446 (2017).

[24]G. Enlai, L. Shao-Zhen, Q. Zhao, M.J. Buehler, F. Xi-Qiao, X. Zhiping, Journal of the

Mechanics and Physics of Solids **115**, 248 (2018).

[25]J.D. Caldwell, T.J. Anderson, J.C. Culbertson et al., ACS Nano **4**, 1108 (2010).

[26]Q. Zhang et al., Nature Communications **10**, 727 (2019).

[27]C. Haws, E. Perez, M. Davanco, J.D. Song, K. Srinivasan, L. Sapienza, Applied Physics Letters 120, 081103 (2022).

[28]S.I. Park, O.J. Trojak, E. Lee, J.D. Song, J. Kyhm, I. Han, J. Kim, G.-C. Yi, L. Sapienza, Nanotechnology **29**, 205602 (2018).

[29]J. Liu, R. Su, Y. Wei et al., Nature Nanotechnology **14**, 586 (2019).

[30]Y. Ma, G. Ballesteros, J.M. Zajac, J. Sun, B.D. Gerardot, Optics Letters **40**, 2373 (2015).

[31]M.R. Gonalves, H. Minassian, A. Melikyan, J. Phys. D: Applied Physics **53**, 443002 (2020).

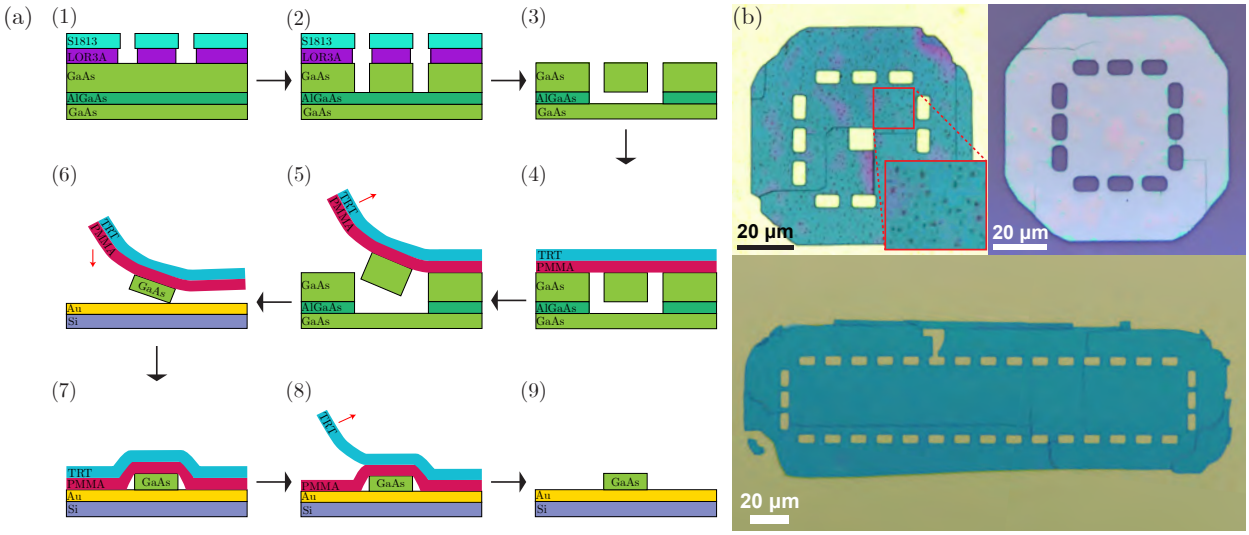


FIG. 1. (a) Schematic (not to scale) of the membrane transfer process used to realise hybrid devices. (1) A direct laser write is used to write a set of of apertures (the holes appear as 'dashed lines' that define the perimeter of the membranes that will be transferred) on a resist layer. (2) The apertures are then dry etched through the GaAs top layer to reach the AlGaAs sacrificial layer. (3) A hydrofluoridic acid wet etch is then used to undercut the membranes. (4) Resist (PMMA) is then deposited on the chip to protect the GaAs from impurities during the transfer process that is carried out by placing a thermal release tape (TRT) on the sample surface. (5) The tape, that has now the membranes attached, is manually removed (6) and placed on a host substrate (7). (8) The tape is heated so that it loses adhesion and leaves the membranes on the host substrate where they are held in place by van der Waals forces. (9) The resist layer that protected the GaAs membrane is then chemically removed with a solvent. (b) Images of membranes transferred using the technique described in (a). The top left (right) panel shows a membrane transferred without (with) the resist protective layer (step 4 in panel (a)): tape residues are visible on the surface of the membrane on the left, while the surface of the membrane on the right appears clean.

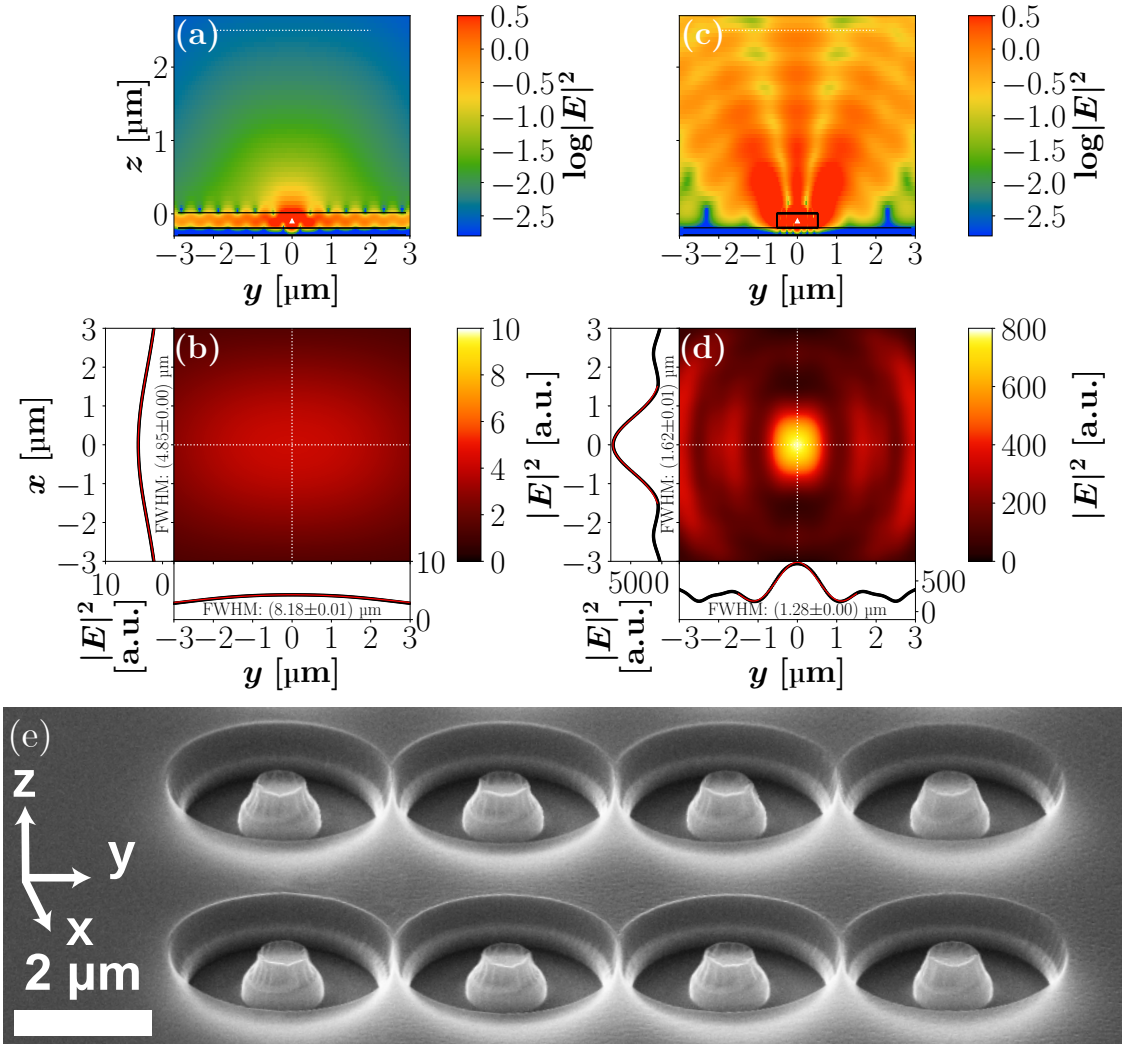


FIG. 2. (a) Colour plot, obtained by finite-difference time-domain simulations, of the side ($zy$ plane) profile of the squared electric field of a dipole emitter (oriented along the $x$ axis and emitting between 925 nm and 975 nm) placed in the middle of a 190 nm-thick GaAs membrane transferred to a Au layer, and (b) top view ($xy$ plane), measured at a distance of 2.5 $\mu$m from the sample surface in correspondence to the dotted line shown in panel (a), including linecuts of the far-field profile (black lines) and their Gaussian fits (red lines). The Full-Width Half-Maximum (FWHM) obtained from the fits is indicated in the graphs, with the error obtained from the fitting function (one standard deviation uncertainty due to the fit negligible compared to the values). (c, d) Same as panels (a, b) in the presence of a micro-pillar with diameter of 1 $\mu$m on the sample surface, centered around the emitting dipole. (e) Scanning electron micrograph image of GaAs micro-pillars (with remnant resist) fabricated via ion milling after deposition, exposure and development of electron-beam resist.

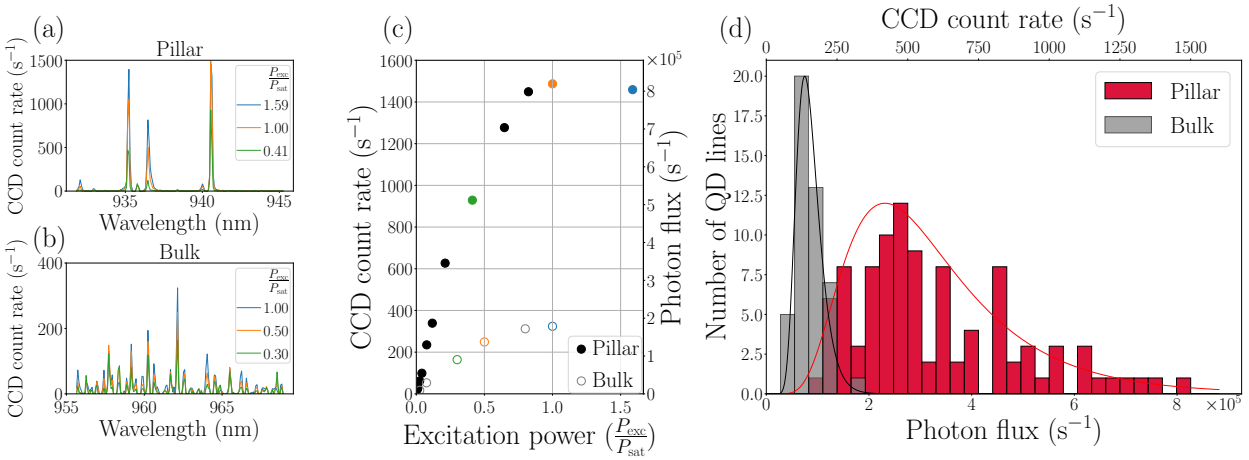


FIG. 3. (a,b) Example of photoluminescence spectra (taken at a temperature of $\approx$ 4 K) of quantum dots placed within (a) and outside (b) micro-pillars, respectively. The photoluminescence is collected using an objective with a numerical aperture of 0.9 and directed to a Charge-Coupled Device (CCD) placed at the exit of a 0.5 m-long spectrometer, (c) Photoluminescence intensity of the emission lines with wavelength of 940.55 nm in panel (a) and 962.14 nm in panel (b) (colour coded accordingly), as a function of excitation power of a continuous wave 780 nm laser ($P_{exc}$), normalised to the power giving the highest emission count rate for a specific emission line ($P_{sat}$ of 170 $\mu$W and 400 $\mu$W, respectively). The photon flux corresponds to the number of single photons collected by the objective per unit time, once taking into consideration the losses in the collection path and the sensitivity of the detectors (correction factor of 550). (d) Statistics of the collected emission intensity for quantum dots in bulk (outside the micro-pillars, about 50 lines) and within micro-pillars (about 100 lines), gray and red histograms respectively. The solid lines are log-normal fits to the histograms.